SERBIAN JOURNAL OF ELECTRICAL ENGINEERING
Vol. 17, No. 2, June 2020, 171-186

UDC: 621.396.21:621.391.812 **DOI: https://doi.org/10.2298/SJEE2002171T**

Analysis of Signal Quality in FSO Systems with PolSK Modulation

Jelena Todorović[1], Branimir Jakšić[1], Petar Spalević[1], Đoko Banđur[1], Miloš Banđur[1]

Abstract: In this paper, the quality of the Polarization Shift Keying (PolSK) modulated signal in a Free Space Optical (FSO) system is analyzed. The atmospheric channel is statistically modeled with four different distributions, namely, the Gamma-Gamma distribution, Negative Exponential distribution, K-distribution, and I-K distribution. For all four channel models, the Average Bit Error Rate (ABER) at the receiving side of the system is determined in an analytically closed form. The results are graphically presented and discussed in order to determine the impact of certain parameters on the ABER, i.e., the quality of the received signal in the PolSK modulated FSO system. These parameters are the Signal-to-Noise Ratio (SNR), the FSO link distance, the wavelength at which the signal is transmitted, and the atmospheric turbulence strength.

Keywords: Average Bit Error Rate (ABER), Channel model, Free Space Optical (FSO), Polarization Shift Keying (PolSK), Signal-to-Noise Ratio (SNR).

1 Introduction

In order to find an alternative to radio frequency (RF) communication, a novel optical wireless communication technique known as Free Space Optical (FSO) communication has been invented. Compared to RF systems, optical wireless communication systems are more resistant to interference. In addition, they provide a higher level of security and use a powerful local receiving oscillator that reduces the effect of noise [1 – 3].

FSO systems are very vulnerable to atmospheric conditions. Atmospheric turbulence has a strong impact on the operating wavelengths of the system. Turbulences are caused by fluctuations in the index of refraction along the propagation path. These atmospheric effects along the signal propagation path can cause phenomena such as beam spreading, image dancing, beam wander,

[1]Univerity of Priština in Kosovska Mitrovica, Faculty of Tehnical Sciences, Kneza Milosa 7, 38220 Kosovska Mitrovica, Serbia; E-mails: jelena.todorovic@pr.ac.rs; branimir.jaksic@pr.ac.rs; petar.spalevic@pr.ac.rs; djoko.bandjur@pr.ac.rs, milos.bandjur@pr.ac.rs

and scintillation, thereby leading to signal degradation and high Bit Error Rate (BER) values for the FSO system [3 – 8].

Thus, it is very important for wireless communications to know the Channel State Information (CSI) first, which refers to the known channel properties of a communication link. Principally, wireless nodes need channel estimation to perform essential tasks, such as precoding, beamforming, and data detection. Channel parameters include channel statistics, such as means and variances, and instantaneous CSI or packet transmission time delays. These are parameters that represent effects such as fading and power decay with distance. A comprehensive analysis on obtaining CSI in the emerging system architecture, Heterogeneous Cloud Radio Access Networks (H-CRANs), is given in [9].

Many distributions have been proposed for modeling different levels of channel atmospheric turbulence. How reliable the connection is depends on the link length and the aperture diameter. The higher the strength of the atmospheric turbulence, the link is available at a shorter distance. Link availability at longer lengths can be achieved by increasing the aperture diameter or using a relay technique [10].

The Gamma-Gamma distribution is usually used for modeling weak to strong turbulence conditions. The main advantage of this model is that it operates under the effect of sub-channel correlation, where other channels do not perform better [10].

The Negative Exponential and K distributions are used for modeling atmospheric channels in strong atmospheric turbulence, while the I-K distribution is suitable for weak and strong atmospheric turbulence [5, 11].

The Negative Exponential distribution can be used to communicate over distances of several kilometers. In this case, for larger values of the average electrical SNR, the average BER decreases and the capacity increases [11]. In the case of strong atmospheric fluctuations where the link length reaches several kilometers, the number of independent scatter becomes large in fading [12].

The K distribution reduces to the Negative Exponential distribution as the value of α tends to infinity [11]. The K distribution is suitable for strong turbulent modes where the scintillation index is nearly 1 and then the value of intensity variance is between 3 and 4. The K distribution channel model is suitable to achieve a distance of 1 km with a SNR ranging from 20 to 27 dB [10, 12].

The I-K distribution is a generalized form of the K distribution that can be used for all atmospheric turbulence conditions, including weak turbulence for which the K distribution is not theoretically applicable. Here, the important parameter, ρ, is considered as a product of two independent models, namely, the Exponential distribution and Gamma distributions. Thus, it can provide the

benefits of both of the models. The main advantage of the I-K distribution model is that the parameters can be easily controlled. Therefore, it is particularly useful when the K distribution is not very experimental [10].

Depending on their detection, there are two types of FSO systems. One of them is intensity modulation/direct detection (IM/DD), which is the main mode of detection in FSO systems. However, as an alternative, coherent communication has also been proposed [13 – 15]. In comparison to IM/DD systems, the implementation of coherent FSO systems is more difficult. Coherent detection is one of the most promising techniques and it offers distinct advantages [15, 16]. It can provide higher receiver sensitivity and improve the channel usage. In addition, it has much better spatial and frequency selectivity because it is based on the use of a local oscillator at the receiver [16, 17]. One of the greatest advantages of coherent systems is the ability to use any kind of amplitude, frequency or phase modulation technique [15, 18].

Polarization Shift Keying (PolSK) is a new digital effective alternative modulation technique in FSO systems with coherent detection. It is used for long-distance wireless optical communications. Compared to other modulation schemes, PolSK provides immunity to atmospheric scintillation, higher data rates and lower BER. It has high immunity to laser phase noise and the light intensity is more uniform when propagating through atmospheric turbulences [14, 19 – 21]. Links in PolSK-based FSO systems have improved performance in terms of peak optical power. Thus, PolSK can be used as an effective method to reduce the impact of turbulence effects [22].

In PolSK, the States of Polarizations (SOPs) of an optical signal are used as information carrying parameters [21]. The information is encoded with different SOPs using an external modulator. PolSK uses intensity modulation, where two orthogonal polarization directions are used for the transmission of 0 and 1 data bits. Thus, the data bits in x and y polarizations are always complementary [14, 23, 24]. In relation to the amplitude and phase in the actual case of laser beam propagation, the SOPs have more stable characteristics.

The probability of a conditional BER that depends on the irradiance fluctuation at the receiver for an optical signal transmitted by a FSO system with the PolSK modulation scheme can be expressed as [25]:

$$P_{ec}(I) = \frac{1}{2}\operatorname{erfc}\left(\sqrt{\frac{R^2 P}{2\sigma^2} I}\right), \tag{1}$$

where R is the photodetector responsivity, P is the local oscillator power, and σ^2 represents the variance of the channel noise.

In this paper, the Average BER (ABER) expressions for the Gamma-Gamma distribution, Negative Exponential distribution, K-distribution, and I-K

distribution are derived for a coherent FSO system using the PolSK modulation scheme. In Section 2, the analyzed system model with initial expressions is given and analytical expressions for the ABER for all four above-mentioned distributions are derived and presented. The obtained numerical results are presented and discussed in Section 3 for different levels of atmospheric turbulence, wavelengths and FSO link distances. Section 4 summarizes the conclusions.

2 Analytical Results

The Average BER can be obtained by averaging (1) over the Probability Density Function (PDF) of the irradiance coefficient at the receiver, *I*, according to [25]:

$$P_e = \int_0^\infty P_{ec}(I) f_I(I)\,\mathrm{d}I. \tag{2}$$

In addition, the average Signal-to-Noise Ratio (SNR) at the receiver for the PolSK based FSO system can be defined as [2, 25]:

$$\overline{SNR}(I) = \frac{R^2 PI}{\sigma^2}. \tag{3}$$

2.1 Gamma-Gamma distribution

The PDF for the Gamma-Gamma model is given by the expression [26]:

$$f_I(I) = \frac{2(\alpha\beta)^{\frac{\alpha+\beta}{2}}}{\Gamma(\alpha)\Gamma(\beta)} I^{\frac{\alpha+\beta}{2}-1} K_{\alpha-\beta}\left(2\sqrt{\alpha\beta I}\right), \tag{4}$$

where *I* is the irradiance at the receiver, Γ(·) represents the Gamma function [27, Eq. 8.310], and *Kυ*(·) is the *υ*th-order modified Bessel function of the second kind [27, Eq. 8.432]. The parameters α and β are the effective numbers of small-scale and large-scale eddies of the scattering environment, respectively. These are atmospheric turbulence parameters that for plane waves propagation and the zero inner scale can be expressed as [26]:

$$\alpha = \left[\mathrm{e}^{\frac{0.49\sigma_R^2}{\left(1+1.11\sigma_R^{12/5}\right)^{7/6}}} - 1 \right]^{-1}, \tag{5}$$

$$\beta = \left[\mathrm{e}^{\frac{0.51\sigma_R^2}{\left(1+0.69\sigma_R^{12/5}\right)^{5/6}}} - 1 \right]^{-1}, \tag{6}$$

where σ_R^2 represents the Rytov variance used to determine the optical signal intensity due to atmospheric turbulence, as defined by:

$$\sigma_R^2 = 1.23 C_n^2 k^{7/6} L^{11/6}. \tag{7}$$

The parameter C_n^2 denotes the index of refraction used as a measure of the turbulence strength. For the horizontal propagation path, the parameter C_n^2 is considered constant with mean values from 10^{-17} $m^{-2/3}$ to 10^{-13} $m^{-2/3}$ for channels from weak to strong turbulence, respectively. The parameter k is an optical wave number, defined as $k = 2\pi/\lambda$ with wavelength λ, while L is the distance between the transmitter and the receiver, i.e., the length of the optical signal propagation.

In order to derive a closed-form ABER expression, the modified Bessel function of the second kind $K\upsilon(\cdot)$ in (4) is represented by the Meijer G function as [27, Eq. 9.34.3]:

$$K_{\nu}(x) = \frac{1}{2} G_{0,2}^{2,0}\left[\frac{x^2}{4} \middle| \begin{matrix} - \\ (\nu-2),\ -(\nu-2) \end{matrix} \right], \tag{8}$$

and the complementary error function $\mathrm{erfc}(\cdot)$ in (1) is represented by the Meijer G function as [28, Eq. 06.27.26.0006.01]:

$$\mathrm{erfc}\left(\sqrt{x}\right) = \frac{1}{\sqrt{\pi}} G_{1,2}^{2,0}\left[x \middle| \begin{matrix} 1 \\ 0,\ 1/2 \end{matrix} \right]. \tag{9}$$

By substituting (4) into (2), we obtain the expression (A1) and then after making use of the relationships given in (8) and (9), the resulting integral (A2) is obtained. By using the solution of the resulting integral given by [29, Eq. 07.34.21.0011.01], we derive the ABER closed form expression as follows:

$$P_e = \frac{(\alpha\beta)^{\frac{\alpha+\beta}{2}}}{2\sqrt{\pi}\Gamma(\alpha)\Gamma(\beta)} \left(\frac{R^2 P}{2\sigma^2} \right)^{-\frac{\alpha+\beta}{2}} G_{2,3}^{2,2}\left[\frac{2\alpha\beta\sigma^2}{R^2 P} \middle| \begin{matrix} 1-\frac{\alpha+\beta}{2},\ \frac{1}{2}-\frac{\alpha+\beta}{2} \\ \frac{\alpha-\beta}{2},\ -\frac{\alpha-\beta}{2},\ -\frac{\alpha+\beta}{2} \end{matrix} \right]. \tag{10}$$

2.2 Negative exponential distribution

The PDF for the Negative Exponential model is given by the expression [11, 30]:

$$f_I(I) = \frac{1}{I_0} \mathrm{e}^{-\frac{I}{I_0}}, \tag{11}$$

where I_0 is the mean irradiance.

By substituting (11) into (2), we obtain the expression (A3) and then after using the relationship given in (9) and the identity [31, Eq. 8.4.3]:

$$e^{-x} = G_{0,1}^{1,0}\left[x \middle| \begin{matrix} - \\ 0 \end{matrix} \right], \tag{12}$$

the resulting integral (A4) is obtained. By using the solution of the resulting integral given by [29, Eq. 07.34.21.0011.01], we derive the ABER expression as follows:

$$P_e = \frac{2\sigma^2}{2\sqrt{\pi}R^2 P I_0} G_{2,2}^{1,2}\left[\frac{2\sigma^2}{R^2 P I_0}\middle| \begin{matrix} 0, & -\frac{1}{2} \\ 0, & -1 \end{matrix}\right]. \tag{13}$$

2.3 K distribution

The K distribution represents a product of the Exponential and Gamma distributions [11]. The K distribution of the irradiance at the receiver is given by [30]:

$$f_I(I) = \frac{2\alpha^{\frac{\alpha+1}{2}}}{\Gamma(\alpha)} I^{\frac{\alpha-1}{2}} K_{\alpha-1}\left(2\sqrt{\alpha I}\right), \tag{14}$$

where the parameter α is defined by (5).

By substituting (14) into (2), we obtain the expression (A5) and then after using the relationships given in (8) and (9), the resulting integral (A6) is obtained. By using the solution of the resulting integral given by [29, Eq. 07.34.21.0011.01], we derive the ABER expression as follows:

$$P_e = \frac{\alpha^{\frac{\alpha+1}{2}}}{2\sqrt{\pi}\Gamma(\alpha)}\left(\frac{R^2 P}{2\sigma^2}\right)^{-\frac{\alpha+1}{2}} G_{2,3}^{2,2}\left[\frac{2\alpha\sigma^2}{R^2 P}\middle| \begin{matrix} -\frac{\alpha-1}{2}, & -\frac{\alpha}{2} \\ \frac{\alpha-1}{2}, & -\frac{\alpha-1}{2}, & -\frac{\alpha+1}{2} \end{matrix}\right]. \tag{15}$$

2.4 I-K distribution

A generalized form of the K distribution applicable to all atmospheric turbulence conditions, including weak turbulence for which the K distribution is not suitable, is the I-K distribution. For the I-K distribution, the field of the optical wave is modeled as the sum of a coherent (deterministic) component and a random component [11].

The I-K distribution of the irradiance at the receiver is given by [30]:

$$f_I(I) = \begin{cases} 2\alpha(1+\rho)\left(1+\frac{1}{\rho}\right)^{\frac{\alpha-1}{2}} I^{\frac{\alpha-1}{2}} K_{\alpha-1}\left(2\sqrt{\alpha\rho}\right) I_{\alpha-1}\left(2\sqrt{\alpha(1+\rho)I}\right), & 0 < I < \frac{\rho}{1+\rho}, \\ 2\alpha(1+\rho)\left(1+\frac{1}{\rho}\right)^{\frac{\alpha-1}{2}} I^{\frac{\alpha-1}{2}} I_{\alpha-1}\left(2\sqrt{\alpha\rho}\right) K_{\alpha-1}\left(2\sqrt{\alpha(1+\rho)I}\right), & I > \frac{\rho}{1+\rho}, \end{cases} \tag{16}$$

where ρ is the coherence parameter and $I\upsilon(\cdot)$ is the υth-order modified Bessel function of the first kind [27, Eq. 8.431]. The parameter α is defined by (5).

By substituting (16) into (2) for $0 < I < \rho/(1+\rho)$, we obtain the expression (A7) and then after making use of the relationship given in (9) and expressing the modified Bessel function of the first kind $I\upsilon(\cdot)$ in (16) in the form of an infinite series [27, Eq. 8.445]:

$$I_v(x) = \sum_{n=0}^{\infty} \frac{1}{n!\Gamma(v+n+1)} \left(\frac{x}{2}\right)^{v+2n}, \tag{17}$$

the resulting integral (A8) is obtained. By using the solution of the resulting integral given by [27, Eq. 7.811.4], we derive the ABER expression as follows:

$$P_e = \sum_{n=0}^{\infty} \frac{1}{\sqrt{\pi} n!} \frac{\Gamma\left(\alpha+n+\frac{1}{2}\right)}{\Gamma(\alpha+n+1)} \left(\alpha(1+\rho)\right)^{\frac{\alpha+1}{2}+n} \left(1+\frac{1}{\rho}\right)^{\frac{\alpha-1}{2}} \times \\ \times \left(\frac{R^2 P}{2\sigma^2}\right)^{-(\alpha+n)} K_{\alpha-1}\left(2\sqrt{\alpha\rho}\right). \tag{18}$$

By substituting (16) into (2) for $I > \rho/(1+\rho)$, we obtain the expression (A9) and then after using the relationships given in (8) and (9), the resulting integral (A10) is obtained. By using the solution of the resulting integral given by [29, Eq. 07.34.21.0011.01], we derive the ABER expression as follows:

$$P_e = \frac{1}{2\sqrt{\pi}} \alpha(1+\rho) \left(1+\frac{1}{\rho}\right)^{\frac{\alpha-1}{2}} \left(\frac{R^2 P}{2\sigma^2}\right)^{-\frac{\alpha+1}{2}} I_{\alpha-1}\left(2\sqrt{\alpha\rho}\right) \times \\ \times G_{2,3}^{2,2}\left[\frac{2\sigma^2\alpha(1+\rho)}{R^2 P}\middle| \begin{matrix} -\frac{\alpha-1}{2}, & -\frac{\alpha}{2} \\ \frac{\alpha-1}{2}, & -\frac{\alpha-1}{2}, & -\frac{\alpha+1}{2} \end{matrix}\right]. \tag{19}$$

3 Numerical Results

Based on the obtained closed form analytical expressions for atmospheric channels modeled with Gamma-Gamma distribution, Negative Exponential distribution, K distribution, and I-K distribution, i.e., (10), (13), (15), and (19), respectively, the ABER as a function of the SNR and FSO link distance, L, are graphically presented. The FSO system is considered at three different wavelengths: $\lambda = 850$ nm, $\lambda = 1350$ nm and $\lambda = 1550$ nm, as well as three types of atmospheric turbulence: strong, moderate and weak, with indexes of reflection $C_n^2 = 1.2 \cdot 10^{-13}\ \mathrm{m}^{-2/3}$, $C_n^2 = 2 \cdot 10^{-14}\ \mathrm{m}^{-2/3}$ and $C_n^2 = 6 \cdot 10^{-15}\ \mathrm{m}^{-2/3}$, respectively.

3.1 Gamma-Gamma distribution

In Fig. 1 and Fig. 2 is shown the ABER behavior of the FSO channel modeled with the Gamma-Gamma distribution, as a function of the SNR and the link distance.

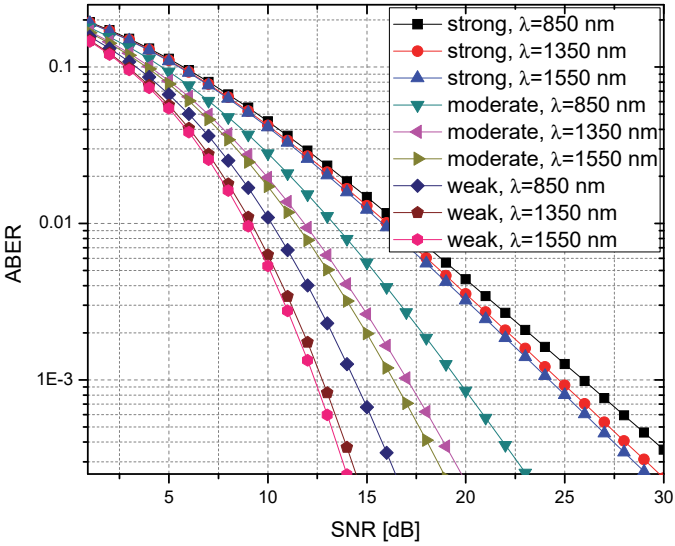

Fig. 1 – *ABER for Gamma-Gamma distribution as a function of SNR.*

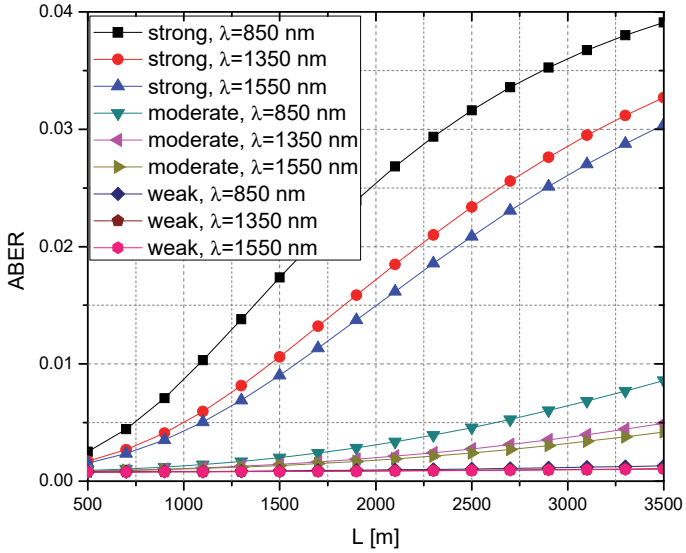

Fig. 2 – *ABER for Gamma-Gamma distribution as a function of link distance L (SNR = 10 dB).*

From Fig. 1, it can be seen that better transmission quality is achieved for higher wavelength values. Furthermore, in the case of stronger atmospheric turbulence, the ABER decreases slower with the increase of the SNR than is the case of moderate and weak atmospheric turbulence.

It can be seen from Fig. 2 that strong atmospheric turbulence leads to a faster increase of the ABER with a FSO link distance increase. For moderate and weak atmospheric turbulence, the ABER increase is significantly less pronounced. In the first 1000 m of the link, the ABER is almost identical for all wavelengths in the cases of moderate and weak atmospheric turbulence.

3.2 Negative exponential distribution

In Fig. 3 is presented the ABER behavior of the FSO channel modeled with the Negative Exponential distribution as a function of the SNR.

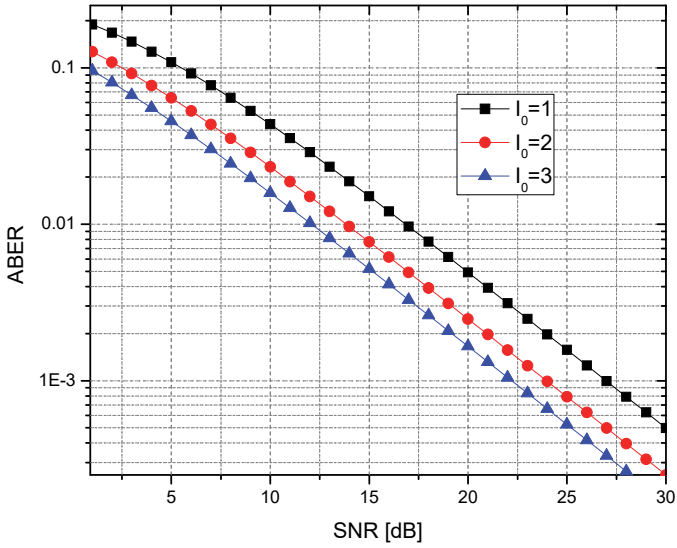

Fig. 3 – *ABER for Negative exponential distribution.*

It can be seen from Fig. 3 that the ABER decreases almost linearly with the increase of the SNR. In addition, from Fig. 3, it can be seen that higher values of the mean irradiance I0 lead to better performance of the FSO system, i.e., lower ABER values.

3.3 K distribution

In Fig. 4 and Fig. 5 is depicted behavior of the ABER for the FSO channel modeled with the K distribution as a function of the SNR and the link distance.It can be seen that for all considered levels of strength of the atmospheric turbulence and wavelengths, similar ABER values are obtained. In

other words, for all considered parameters, the ABER decreases in approximately the same manner with the SNR increase.

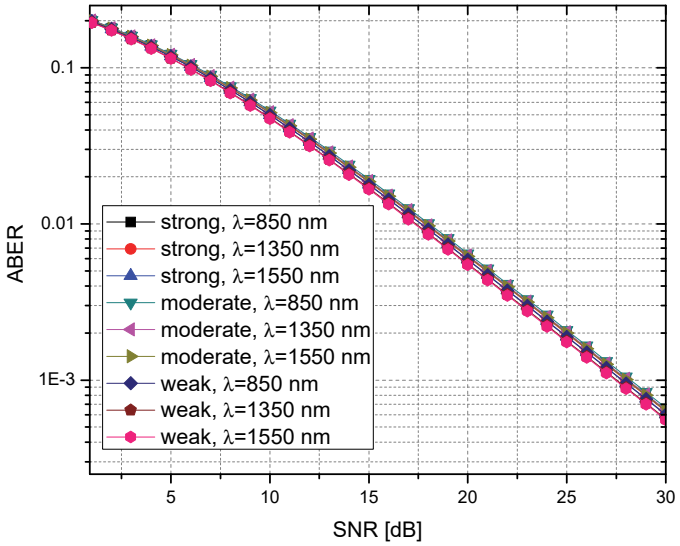

Fig. 4 – *ABER for K distribution as a function of SNR.*

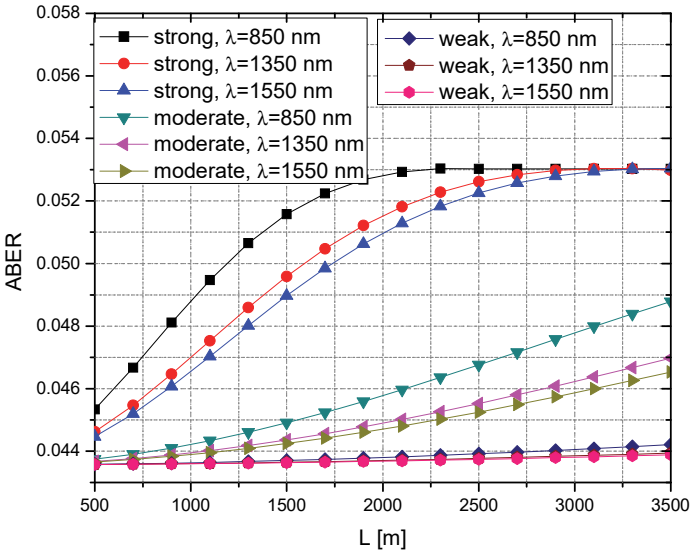

Fig. 5 – *ABER for K distribution as a function of link distance L (SNR* = 10 dB*).*

From Fig. 5, it can be seen that strong atmospheric turbulence leads to a faster increase in the ABER with increasing FSO link distance, similar to the case of channel modeled with the Gamma-Gamma distribution. However, for a

channel modeled with the K distribution, it can be seen that for strong atmospheric turbulence, the ABER tends to be constant for all operating wavelengths. For moderate and weak atmospheric turbulence, the ABER increase is significantly less pronounced. The ABER increase is more pronounced at longer link distances.

3.4 I-K distribution

In Fig. 6 and Fig. 7 is shown the ABER of a FSO channel modeled with the I-K distribution as a function of the SNR and link distance.

From Fig. 6, it can be seen that for SNR<15 dB, approximately the same value of ABER is obtained. It is characteristic for the I-K distribution that for SNR>15 dB, the highest values of ABER are obtained for moderate atmospheric turbulence, and lower values for strong and weak turbulence. This confirms the recommendation that in the case of a moderate level of atmospheric turbulence, the I-K distribution should not be used for FSO channel modelling [9].

From Fig. 7, it can be seen that, for strong atmospheric turbulence, the ABER as a function of the link distance behave identically as the ABER of a channel modeled with the K distribution and tends to a constant value for L>2500 km. In addition, in the case of moderate atmospheric turbulence, the ABER behave similarly as in the case of the channel modeled with the K distribution. In the case of weak atmospheric turbulence, the ABER tends to be approximately constant with FSO link distance changes.

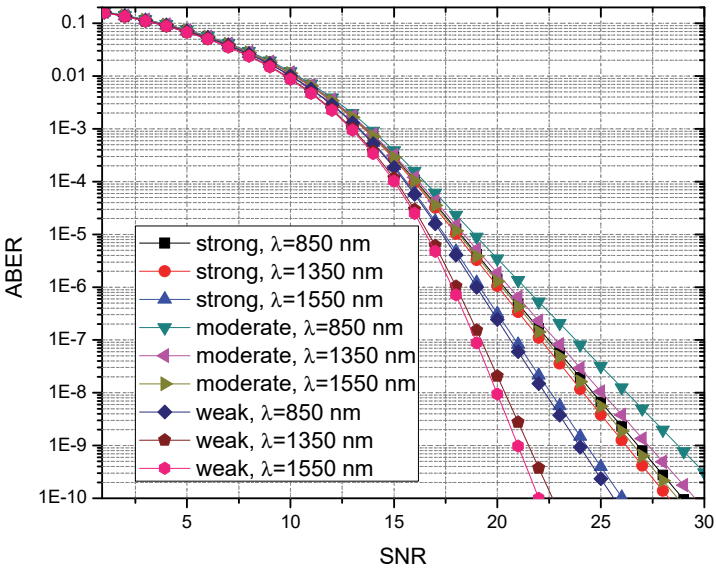

Fig. 6 – *ABER for I-K distribution as a function of SNR.*

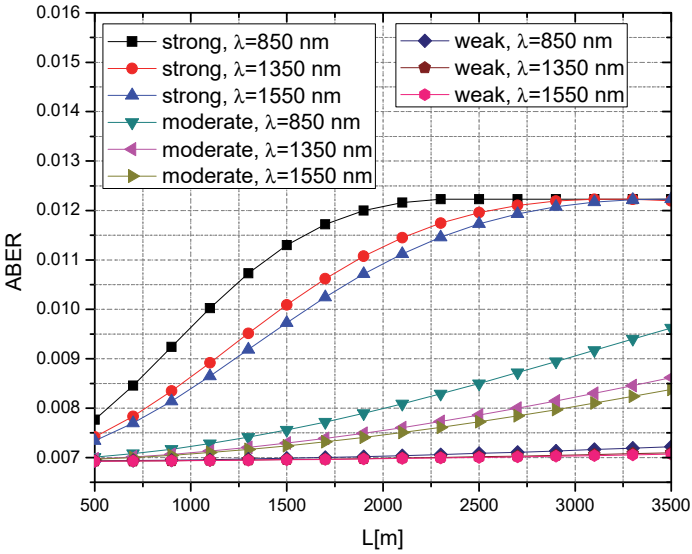

Fig. 7 – *ABER for I-K distribution as a function of link distance L (SNR = 10 dB).*

4 Conclusion

On the basis of the obtained results, it can be seen that the ABER decreases with the SNR increase, that is, increases with the increase in the FSO link distance. The best system performances are obtained for weak atmospheric turbulence and high operating wavelengths, and the worst performances are obtained in the case of strong atmospheric turbulence. The only exception refers to atmospheric channels modeled with the I-K distribution, where the worst performances are obtained for moderate atmospheric turbulence. For that reason, it is not used for FSO channel modelling in the case of a moderate level of atmospheric turbulence. In atmospheric channels modeled with the K distribution, approximately the same value of ABER is obtained for all levels of atmospheric turbulence.

If the behavior of the ABER is considered as a function of the FSO link distance, it can be concluded that in all cases of FSO channel modeling, there is a significant deviation of ABER in cases of strong atmospheric turbulence from other levels of atmospheric turbulence. For channels modeled with Kdistribution and I-K distributions, there is no wavelength impact on the longer link distances (ABER tends to a constant value). Better system performances are achieved for moderate and weak atmospheric turbulence. In these cases, on the shorter sections of the FSO link, there is no wavelength impact on the transmission quality. On the basis of the obtained results, it can be also

concluded that the best performances are obtained for channels modeled with Gamma-Gamma distribution and then for channels modeled with the I-K distribution.

5 Appendix

This Appendix shows the resulting integral expressions for the PDF for all four channel models whose closed form solutions are presented in the paper.

Expressions for the ABER calculation for Gamma-Gamma distribution is given as:

$$P_e = \int_0^\infty \frac{1}{2}\operatorname{erfc}\left(\sqrt{\frac{R^2P}{2\sigma^2}I}\right)\frac{2(\alpha\beta)^{\frac{\alpha+\beta}{2}}}{\Gamma(\alpha)\Gamma(\beta)}I^{\frac{\alpha+\beta}{2}-1}K_{\alpha-\beta}\left(2\sqrt{\alpha\beta I}\right)\mathrm{d}I\,, \tag{A1}$$

and then the resulting integral is obtained:

$$P_e = \frac{(\alpha\beta)^{\frac{\alpha+\beta}{2}}}{2\sqrt{\pi}\Gamma(\alpha)\Gamma(\beta)}\int_0^\infty I^{\frac{\alpha+\beta}{2}-1}G_{1,2}^{2,0}\left[\frac{R^2P}{2\sigma^2}I\middle|\begin{matrix}1\\0,\ \frac{1}{2}\end{matrix}\right]\times$$
$$\times G_{0,2}^{2,0}\left[\alpha\beta I\middle|\begin{matrix}-\\ \frac{\alpha-\beta}{2},\ -\frac{\alpha-\beta}{2}\end{matrix}\right]\mathrm{d}I. \tag{A2}$$

Expressions for the ABER calculation for the Negative exponential distribution is given as:

$$P_e = \int_0^\infty \frac{1}{2}\operatorname{erfc}\left(\sqrt{\frac{R^2P}{2\sigma^2}I}\right)\frac{1}{I_0}\mathrm{e}^{-\frac{I}{I_0}}\,\mathrm{d}I\,, \tag{A3}$$

and then the resulting integral is obtained:

$$P_e = \frac{1}{2\sqrt{\pi}I_0}\int_0^\infty G_{1,2}^{2,0}\left[\frac{R^2P}{2\sigma^2}I\middle|\begin{matrix}1\\0,\ \frac{1}{2}\end{matrix}\right]G_{0,1}^{1,0}\left[\frac{I}{I_0}\middle|\begin{matrix}-\\0\end{matrix}\right]\mathrm{d}I\,. \tag{A4}$$

Expressions for the ABER calculation for the K distribution is given as:

$$P_e = \int_0^\infty \frac{1}{2}\operatorname{erfc}\left(\sqrt{\frac{R^2P}{2\sigma^2}I}\right)\frac{2\alpha^{\frac{\alpha+1}{2}}}{\Gamma(\alpha)}I^{\frac{\alpha-1}{2}}K_{\alpha-1}\left(2\sqrt{\alpha I}\right)\mathrm{d}I\,, \tag{A5}$$

and then the resulting integral is obtained:

$$P_e = \frac{\alpha^{\frac{\alpha+1}{2}}}{2\sqrt{\pi}\Gamma(\alpha)} \int_0^\infty I^{\frac{\alpha-1}{2}} G_{1,2}^{2,0}\left[\frac{R^2 P}{2\sigma^2} I \middle| \begin{matrix} 1 \\ 0,\ \frac{1}{2} \end{matrix}\right] \times G_{0,2}^{2,0}\left[\alpha I \middle| \begin{matrix} - \\ \frac{\alpha-1}{2},\ -\frac{\alpha-1}{2} \end{matrix}\right] \mathrm{d}I\,. \quad \text{(A6)}$$

Expressions for the ABER calculation for the I-K distribution for $0 < I < \rho/(1+\rho)$ is given as:

$$P_e = \int_0^\infty \frac{1}{2}\operatorname{erfc}\left(\sqrt{\frac{R^2 P}{2\sigma^2} I}\right) 2\alpha(1+\rho)\left(1+\frac{1}{\rho}\right)^{\frac{\alpha-1}{2}} I^{\frac{\alpha-1}{2}} \times \\ \times K_{\alpha-1}\left(2\sqrt{\alpha\rho}\right) I_{\alpha-1}\left(2\sqrt{\alpha(1+\rho)I}\right) \mathrm{d}I, \quad \text{(A7)}$$

and then the resulting integral is obtained:

$$P_e = \sum_{n=0}^{\infty} \frac{1}{\sqrt{\pi} n! \Gamma(\alpha+n)} \left(\alpha(1+\rho)\right)^{\frac{\alpha+1}{2}+n} \left(1+\frac{1}{\rho}\right)^{\frac{\alpha-1}{2}} K_{\alpha-1}\left(2\sqrt{\alpha\rho}\right) \times \\ \times \int_0^\infty I^{\alpha+n-1} G_{1,2}^{2,0}\left[\frac{R^2 P}{2\sigma^2} I \middle| \begin{matrix} 1 \\ 0,\ \frac{1}{2} \end{matrix}\right] \mathrm{d}I. \quad \text{(A8)}$$

Expressions for the ABER calculation for the I-K distribution for $I > \rho/(1+\rho)$ is given as:

$$P_e = \int_0^\infty \frac{1}{2}\operatorname{erfc}\left(\sqrt{\frac{R^2 P}{2\sigma^2} I}\right) 2\alpha(1+\rho)\left(1+\frac{1}{\rho}\right)^{\frac{\alpha-1}{2}} I^{\frac{\alpha-1}{2}} \times \\ \times I_{\alpha-1}\left(2\sqrt{\alpha\rho}\right) K_{\alpha-1}\left(2\sqrt{\alpha(1+\rho)I}\right) \mathrm{d}I, \quad \text{(A9)}$$

and then the resulting integral is obtained:

$$P_e = \frac{1}{2\sqrt{\pi}} \alpha(1+\rho)\left(1+\frac{1}{\rho}\right)^{\frac{\alpha-1}{2}} I_{\alpha-1}\left(2\sqrt{\alpha\rho}\right) \times \\ \times \int_0^\infty I^{\frac{\alpha-1}{2}} G_{1,2}^{2,0}\left[\frac{R^2 P}{2\sigma^2} I \middle| \begin{matrix} 1 \\ 0,\ \frac{1}{2} \end{matrix}\right] G_{0,2}^{2,0}\left[\alpha(1+\rho) I \middle| \begin{matrix} - \\ \frac{\alpha-1}{2},\ -\frac{\alpha-1}{2} \end{matrix}\right] \mathrm{d}I. \quad \text{(A10)}$$

5 References

[1] K. Prabu, S. Thakkar: Analysis of FSO Link with Time Diversity over M-Distribution Channel Model with Pointing Errors and GVD Effects, Optics Communications, Vol. 421, August 2018, pp. 115 – 124.

[2] G. Aarthi, G.R. Reddy: Average Spectral Efficiency Analysis of FSO Links over Turbulence Channel with Adaptive Transmissions and Aperture Averaging, Optics Communications, Vol. 410, March 2018, pp. 896 – 902.

[3] I.K. Son, S. Mao: A Survey of Free Space Optical Networks, Digital Communications and Networks, Vol. 3, No. 2, November 2016, pp. 67 – 77.

[4] M.B. El Mashade, A. H. Toeima: Performance Characterization of Spatial Diversity Based Optical Wireless Communication over Atmospheric Turbulence Channels, Radioelectronics and Communications Systems, Vol. 61, No. 4, May 2018, pp. 135 – 152.

[5] S. Malik, P.K. Sahu: Performance Analysis of Free Space Optical Communication System Using Different Modulation Schemes over Weak to Strong Atmospheric Turbulence Channels, Optical and Wireless Technologies, April 2019, pp. 387 – 399.

[6] K. Prabu: Analysis of FSO Systems with SISO and MIMO Techniques, Wireless Personal Communications, Vol. 105, No. 3, February 2019, pp. 1133 – 1141.

[7] G.K. Varotsos, H.E. Nistazakis, C.K. Volos, G.S. Tombras: FSO Links with Diversity Pointing Errors and Temporal Broadening of the Pulses over Weak to Strong Atmospheric Turbulence Channels, Optik - International Journal for Light and Electron Optics, Vol. 127, No. 6, March 2016, pp. 3402 – 3409.

[8] H. Henniger, O. Wilfert: An Introduction to Free-Space Optical Communications, Radioengineering, Vol. 19, No. 2, June 2010, pp. 203 – 212.

[9] G. Wang, Q. Liu, R. He, F. Gao, C. Tellambura: Acquisition of Channel State Information in Heterogeneous Cloud Radio Access Networks: Challenges and Research Directions, IEEE Wireless Communications, Vol. 22 , No. 3 , June 2015, pp. 100 – 107.

[10] E. Jarangal, D. Dhawan: Comparison of Channel Models based on Atmospheric Turbulences of FSO System- A Review, International Journal of Research in Electronics and Computer Engineering, Vol. 6, No. 1, March 2018, pp. 282 – 286.

[11] K. Anbarasi, C. Hemanth, R.G. Sangeetha: A Review on Channel Models in Free Space Optical Communication Systems, Optics and Laser Technology, Vol. 97, December 2017, pp. 161 – 171.

[12] D. Shah, B. Nayak, D. Jethawani: Study of Different Atmospheric Channel Models, International Journal of Electronics and Communication Engineering & Technology (IJECET), Vol. 5, No. 1, January 2014, pp. 105 – 112.

[13] I.S. Ansari, F. Yilmaz, M.- S. Alouini: Performance Analysis of Free-Space Optical Links over Malaga Turbulence Channels with Pointing Errors, IEEE Transactions on Wireless Communications, Vol. 15, No. 1, January 2016, pp. 91 – 102.

[14] J. Zhang, Z. Li, A. Dang: Performance of Wireless Optical Communication Systems under Polarization Effects over Atmospheric Turbulence, Optics Communications, Vol. 416, June 2018, pp. 207 – 213.

[15] K.P. Peppas, P.T. Mathiopoulos: Free-Space Optical Communication with Spatial Modulation and Coherent Detection over H-K Atmospheric Turbulence Channels, Journal of Lightwave Technology, Vol. 33, No. 20, October 2015, pp. 4221 – 4232.

[16] S.M. Aghajanzadeh, M. Uysal: Multi-Hop Coherent Free-Space Optical Communications over Atmospheric Turbulence Channels, IEEE Transactions on Communications, Vol. 59, No. 6, June 2011, pp. 1657 – 1663.

[17] R. Li, A. Dang: A Novel Coherent OCDMA Scheme over Atmospheric Turbulence Channels, IEEE Photonics Technology Letters, Vol. 29, No. 5, March 2017, pp. 427 – 430.

[18] J. Park, E. Lee, C.- B. Chae, G. Yoon: Outage Probability Analysis of a Coherent FSO Amplify-and-Forward Relaying System, IEEE Photonics Technology Letters, Vol. 27, No. 11, June 2015, pp. 1204 – 1207.

[19] K. Prabu, S. Cheepalli, D.S. Kumar: Analysis of PolSK Based FSO System Using Wavelength and Time Diversity over Strong Atmospheric Turbulence with Pointing Errors, Optics Communications, Vol. 324, August 2014, pp. 318 – 323.

[20] K. Prabu, D.S. Kumar: Polarization Shift Keying Based Relay-Assisted Free Space Optical Communication over Strong Turbulence with Misalignment, Optics & Laser Technology, Vol. 76, January 2016, pp. 58 – 63.

[21] J. Jeyaseelan, D.S. Kumar, B. E. Caroline: PolSK and ASK Modulation Techniques Based BER Analysis of WDM‑FSO System for Under Turbulence Conditions, Wireless Personal Communications, Vol. 103, No. 4, October 2018, pp. 3221 – 3237.

[22] F. Bai, Y. Su, T. Sato: Performance Analysis of Heterodyne-Detected OCDMA Systems Using PolSK Modulation over a Free-Space Optical Turbulence Channel, Electronics, Vol. 4, No. 4, October 2015, pp. 785 – 798.

[23] Y. Su, F. Bai, T. Sato: Transmission Analysis of CPolM-Based OFDM FSO System in Atmospheric Turbulence, Optics Communications, Vol. 369, June 2016, pp. 111 – 119.

[24] Y. Su, T. Sato: Analysis of CPolSK-Based FSO System Working in Space-to-Ground Channel, Optics Communications, Vol. 410, March 2018, pp. 660 – 667.

[25] K.A. Balaji, K. Prabu: Performance Evaluation of FSO System Using Wavelength and Time Diversity over Malaga Turbulence Channel with Pointing Errors, Optics Communications, Vol. 410, March 2018, pp. 643 – 651.

[26] H.G. Sandalidis, T.A. Tsiftsis, G. K. Karagiannidis: Optical Wireless Communications with Heterodyne Detection over Turbulence Channels with Pointing Errors, Journal of Lightwave Technology, Vol. 27, No. 20, October 2009, pp. 4440 – 4445.

[27] I.S. Gradshteyn, I.M. Ryzhik: Table of Integrals, Series, and Products, 7th Edition, Elsevier Academic Press, San Diego, London, 2007.

[28] The Wolfram Functions Site: Erfc functions. [Online] Available on: http://functions.wolfram.com/PDF/Erfc.pdf

[29] The Wolfarm Functions Site: MeijerG functions. [Online] Available on: http://functions.wolfram.com/PDF/MeijerG.pdf

[30] J. Parikh, V.K. Jain: Study on Statistical Models of Atmospheric Channel for FSO Communication Link, Proceedings of the Nirma University International Conference on Engineering, Ahmedabad, India, December 2011, pp. 1 – 7.

[31] A.P. Prudnikov, Y.A. Brychkov, O.I. Marichev: Integrals and Series, 2nd Edition, Fizmatlit, Moscow, 2003.